

Counter gradient diffusion vs “counter diffusion” temperature profile?

Pierre Paranthoën^{*}, Gilles Godard, Franck Weiss, Michel Gonzalez

LTH, UMR 6614 CNRS, CORIA, BP 12, 76801 Saint Etienne du Rouvray, France

Received 19 March 2003

Abstract

This experimental study is devoted to the diffusion of a passive scalar downstream from a heated line source located on the centre line of a Bénard–von Kármán street. Measurements of velocity and temperature have been performed using LDA and cold wire thermometer. The results show that, in the central part of the thermal plume, the transverse heat flux and transverse mean temperature gradient have always the same sign. The failure of the gradient transport model in the case under study is proved to result from the special shape of the probability density function of transverse velocity fluctuations at the source location.

© 2003 Elsevier Ltd. All rights reserved.

1. Introduction

Recent interest in heat and mass transfer problems with regard to environmental or combustion applications has raised the attention paid to understanding of passive contaminant turbulent transport [1]. In this context, both a proper modelling and accurate measurements of the passive scalar flux are needed. Despite continuous progress in turbulence modelling of scalar transport [2], the passive scalar flux is commonly modelled using a simple Boussinesq-type assumption. By analogy with the eddy viscosity concept, the passive scalar flux $\langle u_i \theta \rangle$ is written as $\langle u_i \theta \rangle = -a_T \partial \langle \Delta \theta \rangle / \partial x_i$, where u_i and θ are, respectively, the velocity and scalar fluctuating parts. $\langle \Delta \theta \rangle$ is the mean scalar value and a_T the turbulent diffusivity.

The latter approach has led to a reasonable degree of success, especially in free shear flows as mentioned by Sreenivasan et al. [3], although the validity criteria of the transport gradient model are never fulfilled in passive

scalar turbulent transport. In particular, the characteristic scales of the turbulent transport mechanism are never much smaller than the characteristic scale of the mean scalar field [4].

Furthermore, several experimental studies have revealed the existence of regions where the transverse turbulent heat flux $\langle v \theta \rangle$ and the mean scalar gradient $\partial \langle \Delta \theta \rangle / \partial y$ have the same sign [3,5–7]. This implies that the principal term in the expression for temperature variance production, i.e. $-\langle v \theta \rangle \partial \langle \Delta \theta \rangle / \partial y$ is negative. This result was exclusively obtained in inhomogeneous flows and ascribed to the major role of large structures in turbulent transport. It was connected with the asymmetry of the mean temperature profile [5], or to the asymmetry of the velocity p.d.f., [7].

A very simple experiment has been carried out in order to study, in a simpler manner, the role of coherent structures in the turbulent transport of a passive scalar as well as the possible existence of regions of counter-gradient flux. The flow considered here is the Bénard–von Kármán street that is, the periodic wake of a circular cylinder at low Reynolds number Re ($48 < Re = U_\infty D / \nu_g < 150$). Here, U_∞ is the free stream velocity, D is the cylinder diameter and ν_g is the kinematic viscosity of the fluid calculated at the free stream temperature. In this flow, a symmetric mean temperature field is generated by using a small heated line source located in

^{*} Corresponding author. Address: Université de Rouen, UMR 6614 CNRS, Mont Saint Aignan Cedex 76821, France. Tel.: +33-2-35-14-65-80; fax: +33-2-32-95-37-98.

E-mail address: pierre.paranthoen@coria.fr (P. Paranthoën).

Nomenclature

a_T	turbulent diffusivity, $\text{m}^2 \text{s}^{-1}$
c_p	specific heat, $\text{J m}^{-1} \text{K}^{-1}$
d	source wire diameter, m
D	main cylinder diameter, m
f	frequency, Hz
l	length, m
l_c	standard deviation of the instantaneous thermal plume, m
$p(\cdot)$	probability density function, $(\cdot)^{-1}$
P	electric power, W
T_L	Lagrangian integral time scale, s
U	streamwise velocity, m s^{-1}
U_c	convection velocity, m s^{-1}
u	coherent streamwise velocity fluctuation, m s^{-1}
V	transverse velocity, m s^{-1}
v	coherent transverse velocity fluctuation, m s^{-1}
x	streamwise coordinate, m
y	transverse coordinate, m

y_c	centroïd, m
Re	Reynolds number
St	Strouhal number

Greek symbols

ρ	density, kg m^{-3}
σ_c	standard deviation of the centroïd, m
ν	kinematic viscosity, $\text{m}^2 \text{s}^{-1}$
$\Delta\theta$	temperature excess with respect to ambient, K
θ	coherent temperature fluctuation, K
Δx	streamwise coordinate (origin at the source), m

Subscripts and superscripts

c	instantaneous plume
∞	free stream
s	source
$\langle \cdot \rangle$	mean value
*	dimensionless
cg	counter gradient

the near wake, on the centreline. The outline of the paper is as follows: in Section 2 the experimental apparatus and experimental techniques are described, the experimental results regarding heat fluxes and temperature field are presented in Section 3 and discussed in Section 4.

2. Experimental set-up

In this experiment, carried out in air, the vortex shedding bluff body is a smooth stainless steel, 2 mm diameter cylinder mounted horizontally in the middle of the potential core of a vertical laminar plane jet with an initial section of $32 \text{ mm} \times 300 \text{ mm}$. The initial turbulence level, measured by hot-wire anemometry, is lower than 0.3%. Parallel shedding is obtained by manipulating the (spanwise) end boundary conditions. The Reynolds number $Re = 63$ ($Re = Re_c + 15$) is obtained with a velocity $U_\infty = 49 \text{ cm/s}$. Here, Re_c is the critical Reynolds number. The corresponding vortex shedding frequency f and Strouhal number $St = fD/U_\infty$ are about 33 Hz and 0.133 respectively.

As shown in Fig. 1, the line source is a $20 \mu\text{m}$ diameter wire set parallel to the cylinder. The cylinder diameter to the source diameter ratio is 100. The source is heated by Joule effect with an electric power per unit length P/l limited to 10 W/m in order to avoid buoyancy effect. The Reynolds and Richardson numbers of the source are lower than 1 and 10^{-3} respectively.

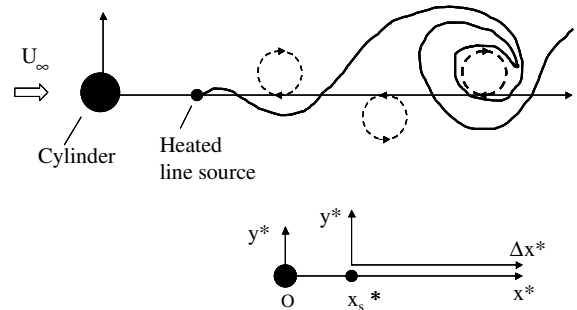


Fig. 1. Experimental set-up.

As shown also in Fig. 1, the x -axis is oriented in the direction of the flow, the y -axis is perpendicular to the flow and the z -axis coincides with the cylinder axis. The Δx axis is in the direction of the flow, with an origin at the source location. U and V are the instantaneous values of longitudinal (along x) and transverse (along y) velocities. $\Delta\theta$ denotes the instantaneous temperature excess with respect to ambient. In our study, the asterisk always denotes normalization. Lengths are normalized by the main cylinder diameter D and velocities by the upstream velocity U_∞ . Temperature differences are normalized by a reference excess temperature $\Delta\theta_{\text{ref}} = P/l\rho c_p U_\infty d$. Each instantaneous quantity (velocity or temperature) is decomposed as the sum of a time mean component ($\langle U \rangle$, $\langle V \rangle$ and $\langle \Delta\theta \rangle$) and a coherent fluctuation (u , v and θ).

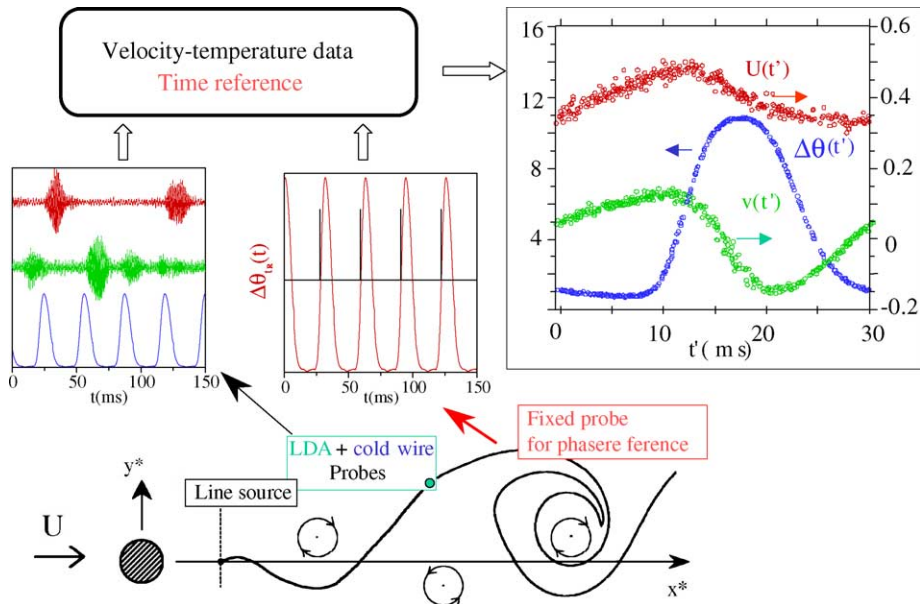


Fig. 2. Block diagram of the phase-averaging method.

The source is located at $x_s^* = 7$, on the centerline ($y_s^* = 0$). At this location, the source is outside the regions where a thin heated wire can control the vortex shedding phenomenon [8,9].

For the present experiment, simultaneous measurements of the longitudinal and transverse velocity components and temperature are made using a two components system LDA TSI in combination with a 1.27 μm diameter cold wire. The LDA measurement volume is $0.08 \times 0.08 \times 2 \text{ mm}^3$ with the major axis parallel to the z -axis. The flow is seeded upstream with olive oil droplets. An other cold wire probe is also used in order to provide a phase reference for the signals from the LDA-cold wire probe. The cold wires are operated with in-house constant current ($I = 0.1 \text{ mA}$) circuits. During the experiment, particular attention is paid to control the frequency cold wire response degradation due to oil particles for LDA measurements [10]. This frequency is always at least 400 Hz beyond 10 times the shedding frequency.

The U , V and $\Delta\theta$ signals from the moving LDA-cold wire probe are recorded and processed by a personal computer. As mentioned above, the following decomposition has been applied to the periodic signals:

$$Q = \langle Q \rangle + q$$

where $\langle Q \rangle$ ($\langle U \rangle$, $\langle V \rangle$ or $\langle \Delta\theta \rangle$) is the time mean component and $q(u, v$ or $\theta)$ is the coherent fluctuation. From this decomposition, it is possible to calculate, using time averaging, moments or cross moments of velocity and

temperature fields. Additional information is obtained by using phase averaging.

The phase-averaging method is based on the sinusoidal temperature signal measured by the second fixed cold-wire. As shown in Fig. 2, when the amplitude of this signal reaches a threshold level, with a positive slope, an electronic circuitry generates a pulse. The instants of time t_i of these pulses allow to record, at each location, the values of the $U(t)$, $V(t)$ and $\Delta\theta(t)$ signals with the same time reference. The phase Φ is then calculated as follows:

$$\Phi = 2\pi(t - t_i)/T_0$$

where $T_0 = 33 \text{ ms}$, the period of vortex shedding is divided into 200 equal time intervals.

3. Experimental results

Figs. 3 and 4 show the transverse distributions of mean temperature excess $\langle \Delta\theta^* \rangle$ and transverse heat flux $\langle v^*\theta^* \rangle$ obtained at distances $\Delta x^* = 1, 2, 4, 8$ and 16 from the source. At each section, the mean temperature profiles are almost symmetric and exhibit local maxima on each side of the centerline. Close to the source, there is a slight asymmetry due to the difficulty to locate the heated line source exactly on the centerline. Clearly, in these figures, the transverse heat flux $\langle v^*\theta^* \rangle$ and the mean temperature gradient $\partial \langle \Delta\theta^* \rangle / \partial y^*$ are of same signs in the central part of the mean plume. This result is more obvious in Figs. 5 and 6 where $-\langle v^*\theta^* \rangle$ is plotted as a

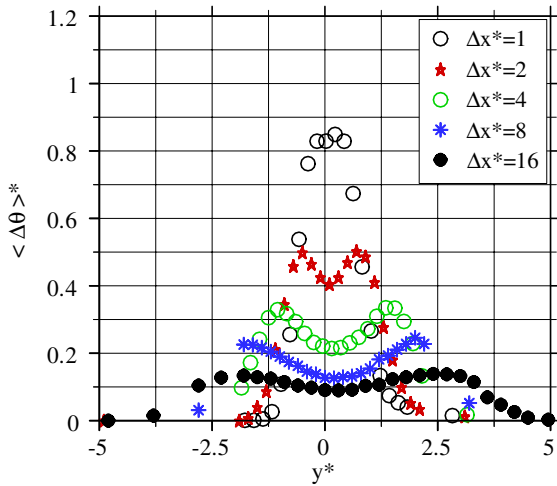


Fig. 3. Mean temperature profiles downstream the heated line source; $\Delta x^* = 1, 2, 4, 8$ and 16 .

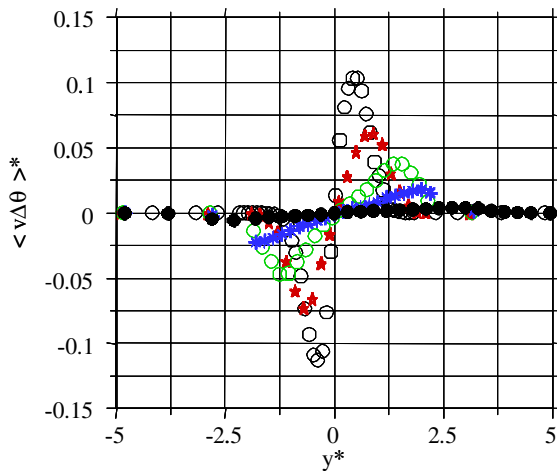


Fig. 4. Transverse heat flux profiles downstream the heated line source; $\Delta x^* = 1, 2, 4, 8$ and 16 . Same symbols as Fig. 3.

function of $\partial\langle\Delta\theta^*\rangle/\partial y^*$ at $\Delta x^* = 2$ and 6 . The experimental points are located on a twisted loop passing through the origin. The experimental points corresponding to the counter-gradient zones belong to the quadrants 2 ($\partial\langle\Delta\theta^*\rangle/\partial y^* < 0, -\langle v^*\theta^*\rangle > 0$) and 4 ($\partial\langle\Delta\theta^*\rangle/\partial y^* > 0, -\langle v^*\theta^*\rangle < 0$). These points are located in the centre of the mean plume.

As mentioned by Sreenivasan et al. [3], if the gradient transport model were valid, this loop would collapse on to a single curve and, for a constant turbulent diffusivity a_T , this curve would be a straight line.

The temperature variance total production term, $P_\theta^* = -v^*\theta^*\partial\langle\Delta\theta^*\rangle/\partial y^* - u^*\theta^*\partial\langle\Delta\theta^*\rangle/\partial x^*$ has been measured. As shown in Fig. 7, these data confirm the exist-

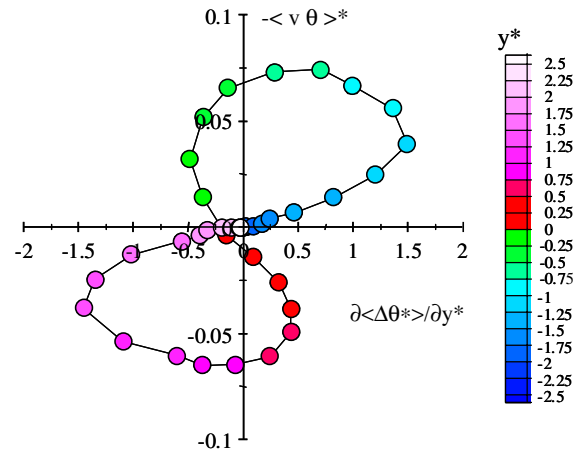


Fig. 5. Transverse heat flux versus mean temperature gradient at $\Delta x^* = 2$.

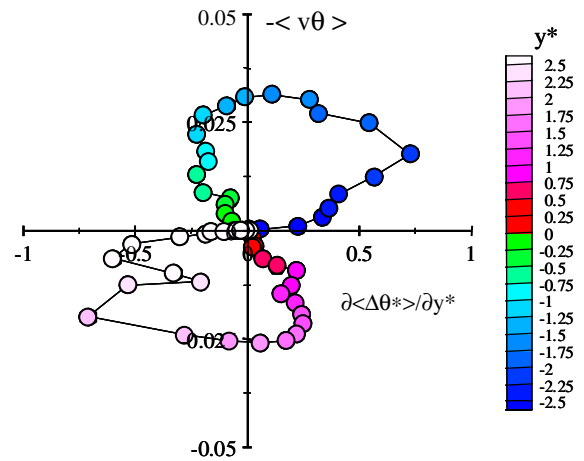


Fig. 6. Transverse heat flux versus mean temperature gradient at $\Delta x^* = 6$.

tence of an important region of “negative production”. The width Δy_{cg}^* of this region is 1.5 at $\Delta x^* = 2$ and 3.3 at $\Delta x^* = 6$. Furthermore, the magnitude of the negative values of the total production is significant since they reach 30–40% of the maximum positive values.

We have proved the existence of this counter-gradient region from mean time measurements. To get additional information, we have studied the time evolution of the instantaneous heat flux $q^* = \rho c_p(iu^*\theta^* + jv^*\theta^*)$, at a given section, as a function of phase. Here i and j are the unit vectors in directions x and y respectively. The result is presented in Fig. 8 at section $\Delta x^* = 4$. The instantaneous fluxes are represented by means of white arrows, the size of which is proportional to the magni-

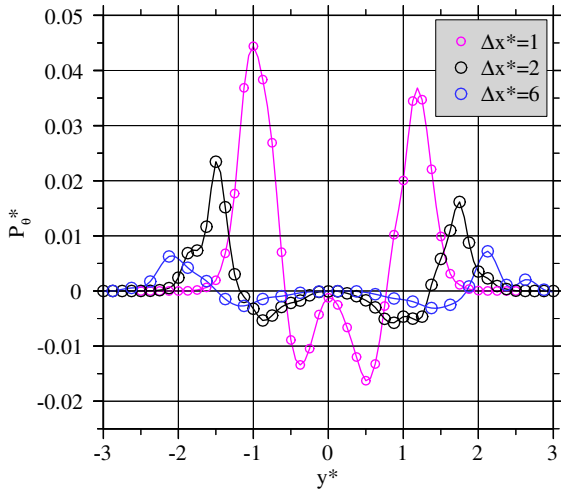


Fig. 7. Profiles of the production terms of the temperature variance equation; $\Delta x^* = 1, 2$ and 6 .

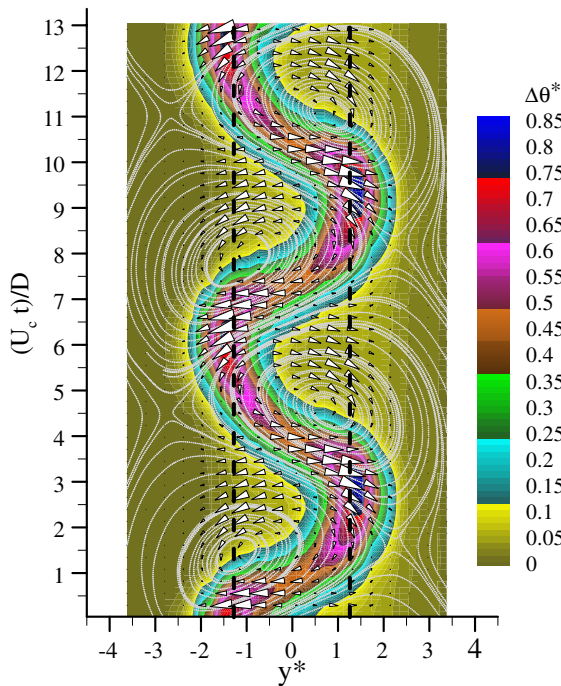


Fig. 8. Instantaneous heat flux versus phase at $\Delta x^* = 4$. Phase calculated with a convection velocity $U_c = 0.85U_\infty$.

tude of the flux. The streamlines are associated to the velocity field $(U^* - U_c^*, v^*)$ where the convection velocity $U_c^* = 0.85$ is obtained from spatio-temporal velocity correlations [17]. In the same figure, the dashed lines are located at the y^* values where the mean temperature gradient $\partial\langle\Delta\theta^*\rangle/\partial y^*$ is zero. In the central part of the

mean plume, the largest heat fluxes are always directed from the centre line toward the edges of the mean plume and follows the mean temperature gradient.

4. Discussion

It is worth noting that, up to now, the existence of counter-gradient zones and the subsequent irrelevance of the gradient transport model have been only mentioned in heated turbulent flows in which the mean temperature profile is asymmetrical [3,5–7,11]. In these experiments, the size of the counter-gradient zone was generally limited and the amount of “negative production” was very weak in comparison with the overall production at the same section. The present experiment shows that the asymmetry of the mean temperature profile or of the mean velocity profile is not a necessary condition for the existence of counter gradient. Results presented in Fig. 7 show also a significant amount of “negative production”.

However, heat flux measurements presented in Fig. 8 do not display any anomalous behaviour. Heat emitted by the source in the centre of the wake is initially transported alternately and symmetrically off the centre line by counter-rotating vortices. It is worth noting that the time averaged heat flux profiles are also very similar to those obtained, close to the source, in similar experiments carried out in turbulent flows [7,12,13].

Actually, in the present conditions, the existence of the counter gradient results from the shape of the mean temperature profile. Close to the source, the flapping model proposed by Lumley and Cruyninghen [14] enables us to calculate the mean temperature distribution. The temperature distribution in the instantaneous plume is assumed to be Gaussian, with a distribution given by,

$$\Delta T(y) = \Delta T_c \exp -(y - y_c)^2 / 2l_c^2 \tag{1}$$

centred on y_c and characterized by a peak value ΔT_c and a standard deviation l_c . The instantaneous centroid y_c has a standard deviation σ_c . The knowledge of its probability density function $p(y_c)$ leads to the mean temperature distribution as,

$$\langle\Delta\theta(y)\rangle = \int \Delta T_c \exp -(y - y_c)^2 / 2l_c^2 p(y_c) dy_c \tag{2}$$

Close to the source, for a convection time t much lower than the Lagrangian integral time scale T_L , the displacement of the centroid y_c of the instantaneous plume is given by vt or, $v\Delta x/U$ [15]. The p.d.f. of y_c is, then, directly related to the p.d.f. of v/U at the source location. Assuming that $l_c \ll \sigma_c$, it results from Eq. (2) that the shape of the mean temperature profile is directly connected to the shape of the probability density function of v/U at the source location [16].

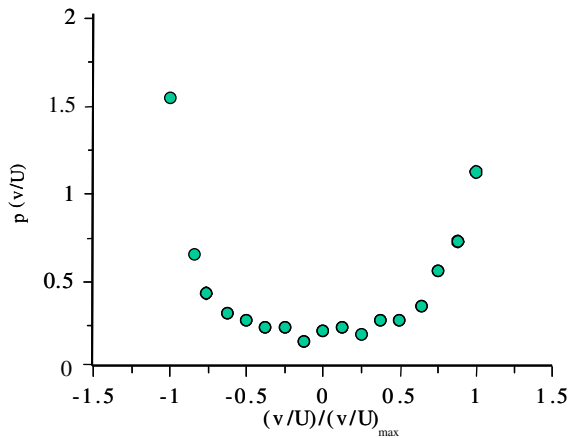


Fig. 9. Probability density function of the intensity of the transverse velocity fluctuation at the source location $y_s^* = 0$.

In fact, this influence of the shape of the p.d.f. of v/U on the shape of the mean temperature distribution occurs whenever $l_s < \sigma_s$. This condition, obtained by Corrsin [4] from the dispersion of an initial Gaussian profile by simple binary random walks, is fulfilled in our experiment.

In the Bénard–von Kármán street, as shown in Fig. 9, the probability density function of v/U , on the centre line at the location of the source, is symmetric and displays two maxima for values $\pm(v/U)_{\max}$. This is implied by the sinusoidal character of the v/U signal due to counter-rotating vortices passing periodically on the centreline. Heat emitted by the source is then rather convected along two trajectories ($x(t) = U_0 t$, $y(t) = \pm(v/U)_{\max} t$), where t is the convective time and U_0 is the value of the streamwise velocity component on the centre line when (v/U) is maximum. This explains the existence of two peaks observed on the mean temperature profiles and located symmetrically on both sides of the centre line.

In the case where the probability density function of v/U is Gaussian, heat is preferentially convected along the centre line. This leads to Gaussian mean temperature distribution and prevents the counter gradient.

The counter gradient results from a rather simple case where blobs of heated flow, of small dimension in comparison with the scale of the velocity field, are convected preferentially along one or two trajectories different from the mean flow direction. This results from the shape of the p.d.f. of v/U . This p.d.f. can be asymmetrical as in the experiment described by Veeravalli and Warhaft [7] or symmetrical as in the present experiment. A necessary condition is that, at the source location, the p.d.f. of v/U be maximum for one or several non zero values of v/U .

It is worth mentioning that, in continuous source experiments, the boundary condition is characterized by

an injection with a constant flux. In this case, where mean temperature profiles are generated by normal convective and diffusive heat transport, it would be more appropriate to characterize these zones as “counter-flux mean temperature profile regions” than as counter-gradient heat flux regions.

5. Conclusion

We have studied experimentally thermal dispersion from a thin heated line source on the centreline of a Bénard–von Kármán street. In this experiment, the profiles of mean temperature and transverse heat fluxes are symmetrical. However, there is a significant region of counter gradient heat flux in the central part of the heated wake. It seems that it is the first time that this result is observed in a heated flow with a symmetrical mean temperature profile. It is shown that this results from the shape of the probability density function of the transverse velocity fluctuation intensity, at the source location, which is maximum for non zero values.

References

- [1] Z. Warhaft, Passive scalars in turbulent flows, *Ann. Rev. Fluid Mech.* 32 (2000) 203–240.
- [2] P.M. Wikström, S. Wallin, A.V. Johansson, Derivation and investigation of a new explicit algebraic model for the passive scalar flux, *Phys. Fluids* 12 (3) (2000) 688–702.
- [3] K.R. Sreenivasan, S. Tavoularis, S. Corrsin, A Test of Gradient Transport and its Generalizations, in: *Turbulent Shear Flows*, vol. 3, Springer-Verlag, 1982, pp. 96–112.
- [4] S. Corrsin, Limitations of gradient transport models in random walks and in turbulence, in: *Adv. Geophys.*, 18A, Academic Press, New York, 1974, pp. 25–60.
- [5] C. Béguier, L. Fulachier, J. Keffer, The turbulent mixing layer with an asymmetrical distribution of temperature, *J. Fluid Mech.* 89 (3) (1978) 561–587.
- [6] G. Charnay, J.P. Schon, E. Alcaraz, J. Mathieu, Thermal characteristics of a turbulent boundary layer with an inversion of wall heat flux, in: *Turbulent Shear Flows*, vol. 1, Springer-Verlag, 1979, pp. 104–118.
- [7] S. Veeravalli, Z. Warhaft, Thermal dispersion from a line source in a shearless turbulence mixing layer, *J. Fluid Mech.* 216 (1990) 35–70.
- [8] P.J. Strykowski, K.R. Sreenivasan, On the formation and suppression of vortex shedding at low Reynolds numbers, *J. Fluid Mech.* 218 (1990) 91–107.
- [9] J.-C. Lecordier, F. Weiss, F. Dumouchel, P. Paranthoën, Contrôle de la transition en aval d’un obstacle 2D au moyen d’une source de chaleur localisée dans son proche sillage, in: Toulouse (Ed.), *Proceedings du Congrès SFT 97*, Elsevier, 1997, pp. 237–242.
- [10] F. Weiss, P. Paranthoën, J.-C. Lecordier, Frequency response of a cold-wire in a flow seeded with oil particles, in: *Proceedings of the 3rd European Thermal Sciences Conference*, Heidelberg, 2000, pp. 665–670.

- [11] L. Fulachier, J. Keffer, C. Béguier, “Production négative” de fluctuations turbulentes de température dans le cas d’un créneau de chaleur s’épanouissant dans une zone de mélange, *Comptes Rendus Acad. Sci. B* 280 (1975) 519–522.
- [12] M. El Kabiri, P. Paranthoën, L. Rosset, J.-C. Lecordier, Fluctuations de température et flux de chaleur en aval d’une source linéaire placée dans une couche limite turbulente, *Revue Générale de Thermique* 37 (1998) 181–194.
- [13] K.R. Raupach, M.R.B.J. Legg, Turbulent dispersion from an elevated line source: measurements of wind-concentration moments and budgets, *J. Fluid Mech.* 136 (1983) 111–137.
- [14] J. Lumley, I. van Cruyninghen, Limitations of second order modeling of passive scalar diffusion, in: *Frontiers in Fluids Mechanics*, Springer Verlag, Berlin, 1985, pp. 199–218.
- [15] G.I. Taylor, Diffusion by continuous movements, *Proc. Lond. Math. Soc.* 2 (20) (1921) 196–211.
- [16] J.O. Hinze, B.G. Van der Hegge Zijnen, *General Discussion on Heat Transfer*, Institute of Mechanical Engineering, London, 1951, pp. 188.
- [17] G. Godard, *Diffusion de la chaleur en présence de structures cohérentes*, Thèse Sci. Phys., Université de Rouen, 2001.